Chloride-Triggered Disproportionation of a Mononuclear Rh^{II}(nbd) Species to Rh^{I}(nbd) and Rh^{III}(η^1-norbornenyl) Complexes: Possibilities for Wacker Type Mono-oxygenation of Norbornadiene to Norbornenone

Dennis G. H. Hetterscheid, Jan M. M. Smits, and Bas de Bruin*

Department of Inorganic Chemistry, University of Nijmegen, Toernooiveld 1, NL-6525 ED Nijmegen, The Netherlands

Received May 14, 2004

Downloaded by NAT LIB UKRAINE on July 6, 2009
Published on July 28, 2004 on http://pubs.acs.org | doi: 10.1021/om049654x

The reactivity of the N_3-ligand rhodium nbd complex [(*fac*-κ^3-Me-dpa)Rh^{I}(nbd)]$^+$ ([**1**]$^+$) toward H^+ and the oxidants Ag^+, $FeCl_3$, and ferrocenium (Fc^+) has been investigated in detail (Me-dpa = *N*-(2-pyridylmethyl)-*N*-(6-methyl-2-pyridylmethyl)amine); nbd = norborna-2,5-diene). The oxidation state +II compound [(*fac*-κ^3-Me-dpa)Rh^{II}(nbd)]$^{2+}$ ([**1**]$^{2+}$) was prepared by one-electron oxidation of [**1**]$^+$ with Ag^+ or Fc^+. EPR spectroscopy and DFT geometry optimizations suggest that [**1**]$^{2+}$ is a square pyramid with the two double bonds of norbornadiene and the two inequivalent pyridyl donors of the *fac*-Me-dpa ligand in the basal plane and the Me-dpa N^{H}_{amine} donor at the apical position. DFT calculations suggest that this conformation may be somewhat stabilized by an agostic interaction between a C−H bond of the Me-dpa methyl group and the Rh^{II} center. Rh^{II}(nbd) complex [**1**]$^{2+}$ is stable in acetone at rt for several hours, but in the presence of water and Cl^- it disproportionates to a 1:1 mixture of [**1**]$^+$ and the η^1-3-hydroxynorbornenyl dinuclear complex [{(*mer*-κ^3-Me-dpa)Rh^{III}(η^1-3-hydroxynorborn-5-en-2-yl)(μ_2-Cl)}$_2$]$^{2+}$ ([**2**]$^{2+}$). This reaction most likely involves external (Wacker type) attack of OH^- to a coordinated double bond of nbd in [**1**]$^{3+}$ or its Cl^- adduct. In MeOH, similar reactivity involving nucleophilic attack of MeO^- to Rh(nbd) is observed, yielding the η^1-3-methoxy-norbornenyl dinuclear complex [{(*mer*-κ^3-Me-dpa)Rh^{III}-(η^1-3-methoxynorborn-5-en-2-yl)(μ_2-Cl)}$_2$]$^{2+}$ ([**3**]$^{2+}$). In contrast to the above nucleophilic attack of OH^- or MeO^- to the coordinated nbd fragment, protonation of [**1**]$^+$ initially occurs at a pyridine group of the Me-dpa ligand, yielding the corresponding square planar complex [(κ^2-Me-dpa*H*)Rh^{I}(nbd)]$^{2+}$ ([**4**]$^{2+}$). In the absence of Cl^-, [**4**]$^{2+}$ is stable, but the presence of Cl^- triggers migration of H^+ from the Medpa*H*$^+$ ligand to the metal and subsequent insertion of a double bond of nbd in the thus obtained Rh^{III}-hydride bond. This *endo* attack of H^+ to the Rh^{I}(nbd) fragment of [**1**]$^+$ results in the formation of the dinuclear η^1-norbornenyl complex [{(*mer*-κ^3-Me-dpa)Rh^{III}(η^1-norborn-5-en-2-yl)(μ_2-Cl)}$_2$]$^{2+}$ ([**5**]$^{2+}$) and contrasts the *exo*-attack of OH^- or MeO^- upon formation of [**2**]$^{2+}$ and [**3**]$^{2+}$. Protonation or nucleophilic attack to other M(nbd) complexes (M = Pd^{II}, Rh^{III}) has invariably resulted in η^3-coordinated norbornenyl derivatives. The (X-ray) structures of [**2**]$^{2+}$ and [**5**]$^{2+}$ are thus unique examples of η^1-coordinated norbonenyl derivatives with a noncoordinated double bond. As a result of this unusual coordination mode, the 3-hydroxynorborn-5-en-2-yl fragment in [**2**]$^{2+}$ undergoes β-elimination to give norbornenone upon heating. In the presence of norbornadiene, [**1**]$^+$ is recovered from this reaction. Thus, these systems offer new possibilities for catalytic oxidation of norbornadiene to norbornenone.

Introduction

Functionalized norbornanes such as norbornenone are valuable synthons in organic synthesis. The synthesis of norbornenone itself however requires several steps from cyclopentadiene and ketene equivalents[1] or stoichiometric oxidation of norbornenol.[2] A catalytic route starting from (commercially available) norbornadiene via Wacker oxidation would be a desirable alternative to produce norbornenone. However, no Wacker oxidation catalysts for norbornadiene have been reported, and oxidation of other diolefins gives poor results or diketones.[3]

Wacker type oxidation usually involves attack of OH^- or H_2O on a Pd^{II} coordinated olefin.[3b] This gives a β-hydroxyalkyl complex, which eliminates the aldehyde (in case of ethene) or methyl ketone (in case of higher

* Corresponding author. Fax: +31 24 355 34 50. E-mail: BdeBruin@sci.kun.nl.

(1) (a) Trost, B. M.; Tamaru, Y. *J. Am. Chem. Soc.* **1977**, *99*, 3101. (b) Aggarwal, V. K.; Jones, D. E.; Martin-Castro, A. M. *Eur. J. Org. Chem.* **2000**, 2939. (c) Aggarwal, V. K.; Anderson, E. S.; Jones, D. E.; Obierey, K. B.; Giles, R. *Chem. Commun.* **1998**, 1985−1986.

(2) Wang, G. T.; Wang, S.; Chen, Y.; Gentles, R.; Sowin, T. *J. Org. Chem.* **2001**, *66*, 2052.

(3) (a) Carlton, L.; Read, G.; Urgelles, M. *J. Chem. Soc., Chem. Commun.* **1983**, 586. (b) Takacs, J. M.; Jiang, X.-T. *Curr. Org. Chem.* **2003**, *7*, 369.

10.1021/om049654x CCC: $27.50 © 2004 American Chemical Society
Publication on Web 07/28/2004

olefins). The classical Wacker catalysis involves *inter*molecular nucleophilic attack (*trans* or *exo* attack) of water (or hydroxide) on a coordinated olefin as the key C−O bond-forming step. However, *intra*molecular (*cis* or *endo* attack, via olefin insertion into a Pd−OH bond) nucleophilic attack is also well documented,[4] and in some cases the two types of attack compete.

The main problem with palladium Wacker oxidation of *di*olefins is that attack of OH^- or H_2O to the Pd^{II}-(diolefin) complex usually yields a η^3-3-hydroxy-enyl $\sigma-\pi$ complex, in which coordination of the second double bond prevents easy β-elimination.[5]

Both examples of *cis*-addition and *trans*-addition of other nucleophiles to Pd^{II}(diolefin) have been reported,[6] as have similar nucleophilic additions to M(diolefin) complexes of platinum,[7] rhodium,[8] and iridium.[9] The mechanistic picture of rhodium-catalyzed olefin oxidation is more complex than that of palladium, with evidence for several mechanisms for various catalysts under different reaction conditions.[3b,10] Nevertheless, many of the proposed reaction mechanisms involve some Wacker steps as part of the overall catalytic cycles.[11] Interestingly, in contrast to Wacker oxidation by palladium, mono-oxygenation of the diolefin 1,5-cyclooctadiene by O_2 to 4-cyclo-octen-1-one is possible with mixtures of $[Rh^{III}(H_2O)_6](ClO_4)_3$/$Cu(ClO_4)_2$/LiCl (1:2:2) in ethanol.[12] To our knowledge, rhodium-catalyzed oxygenation of norbornadiene has not been reported yet. Therefore, we decided to take a closer look at the possibilities for mono-oxygenation of norbornadiene fragments at N_3-ligand Rh^I, Rh^{II}, and Rh^{III} model systems.

In this paper we describe single-electron oxidation of $[(Me\text{-}dpa)Rh^I(nbd)]^+$ to the relatively (air) stable

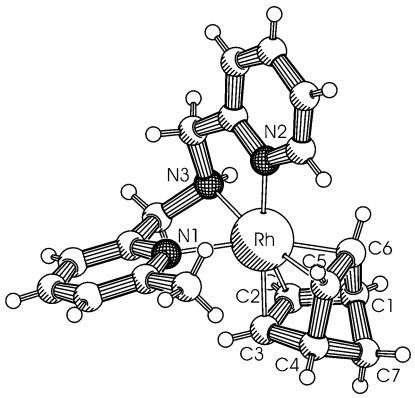

Figure 1. X-ray structure of $[\mathbf{1}]^+$.

Scheme 1. Preparation of Rh^I(nbd) Complex $[\mathbf{1}]PF_6$

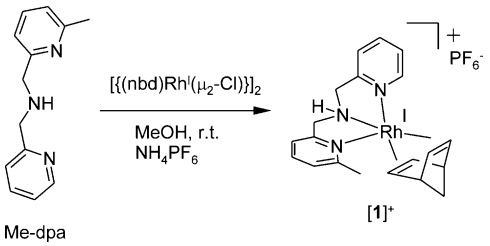

$[(Me\text{-}dpa)Rh^{II}(nbd)]^{2+}$, which is a rare example of an isolated rhodium(II)-olefin species.[13] Disproportionation of this Rh^{II} species (triggered by the presence of Cl^-) and nucleophilic attack at the coordinated nbd fragment then results in unique η^1-coordinated norbornenyl complexes.

Results and Discussion

Synthesis of $[(Me\text{-}dpa)Rh^I(nbd)]^+$. $[(Me\text{-}dpa)Rh^I(nbd)]^+$ ($\mathbf{1}^+$) was prepared by treatment of $[Rh^I(nbd)Cl]_2$ with Me-dpa in methanol. Subsequent treatment with ammonium hexafluorophoshate results in precipitation of $[\mathbf{1}]PF_6$ as a yellow solid (Scheme 1).

Recrystallization of $[\mathbf{1}]PF_6$ in acetone/dioxane yields crystals that were suitable for X-ray diffraction (Figure 1). Selected bond lengths and angles are summarized in Tables 1 and 2. Complex $[\mathbf{1}]^+$ is best described as a trigonal bipyramid with the N2 pyridine and the C2═C3 double bond at the axial positions and the N1 Me-pyridine, the N3 amine and the C5═C6 double bond in the trigonal plane.

For d^8-metals in a trigonal-bipyramidal geometry, theoretical and experimental results by Rossi and Hoffmann indicate that the strongest σ-donor prefers the axial position and that olefins bind more strongly in the trigonal plane.[14] In good agreement, the Rh−C bond distances of the equatorial double bond in $[\mathbf{1}]^+$ are approximately 0.08 Å shorter than those of the axial double bond. The X-ray structure of $[\mathbf{1}]^+$ seems to

(4) See e.g.: Maitlis, P. M.; Espinet, M. J. H. In *Monoolefin and Acetylene Complexes of Palladium in Comprehensive Organometallic Chemistry*; Wilkinson, G., Ed.; Pergamon: Oxford, 1982; Vol. 6, p 357ff.

(5) (a) Donato, E.; Priolo, F. C. *J. Organomet. Chem.* **1983**, *251*, 273. (b) White, D. A. *J. Chem. Soc. A* **1971**, 145. (c) Stille, J. K.; James, D. E. *J. Am. Chem. Soc.* **1975**, *97*, 674.

(6) (a) Hoel, G. R.; Stockland, R. A., Jr.; Anderson, G. K.; Ladipo, F. T.; Bradock-Wilking, J.; Rath, N. P.; Mareque-Rivas, J. C. *Organometallics* **1998**, *17*, 1155. (b) Stockland, R. A.; Anderson, G. K.; Rath, N. P.; Braddockwiling, J.; Ellegood, J. C. *Can. J. Chem.* **1996**, *74*, 1990. (c) Fanizzi, F. P.; Maresca, L.; Natile, G.; Pacifico, C. *J. Chem. Soc., Dalton Trans.* **1994**, 949. (d) Crociani, B.; Dibianca, F.; Uguagliati, P.; Canovese, L.; Baerton, A. *J. Chem. Soc., Dalton Trans.* **1991**, 71. (e) Albéniz, A. C.; Espinet, P.; Jeannin, Y.; Philoche-Levisalles, M.; Mann, B. E. *J. Am. Chem. Soc.* **1990**, *112*, 6594. (f) Segnitz, A.; Bailey, P. M.; Maitlis, P. M. *J. Chem. Soc., Chem. Commun.* **1973**, *18*, 698. (g) Segnitz, A.; Kelly, E.; Taylor, S. H.; Maitlis, P. M. *J. Organomet. Chem.* **1977**, *124*, 113.

(7) (a) Chatt, J.; Vallario, L. M.; Venanzi, L. M. *J. Chem. Soc.* **1957**, 2496. (b) Mulliez, E.; Guillotedelheit, G.; Soulie, J.; Chottard, J. C. *J. Chem. Res., Synop.* **1982**, *6*, 140. (c) Mulliez, E.; Soulie, J.; Chottard, J. C.; Sanchez, C.; Guilhem, J. *J. Chem. Res., Synop.* **1982**, *2*, 38. (d) Giordano, F.; Vitagliano, A. *Inorg. Chem.* **1981**, *20*, L169. (e) Rakowsky, M. H.; Woolcock, J. C.; Rettig, M. F.; Wing, R. M. *Organometallics* **1988**, *7*, 2149.

(8) Hauger, B. E.; Huffman, J. C.; Caulton, K. G. *Organometallics* **1996**, *15*, 1856.

(9) (a) Bresciani-Pahor, N.; Calligaris, M.; Nardin, G.; Delise, P. *J. Chem. Soc., Dalton Trans.* **1976**, 762. (b) Merola, J. S.; Kacmarcik, R. T. *Organometallics* **1989**, *8*, 778. (c) Frazier, J. F.; Anderson, F. E.; Clark, R.; Merola, J. S. *Inorg. Chim. Acta* **1994**, *222*, 135.

(10) de Bruin, B.; Budzelaar, P. H. M.; Gal, A. W. *Angew. Chem., Int. Ed.*, accepted for publication.

(11) (a) Mimoun, H.; Machirant, M. M. P.; Roch, I. *J. Am. Chem. Soc.* **1978**, *100*, 5437. (b) Igersheim, F.; Mimoun, H. *J. Chem. Soc., Chem. Commun.* **1978**, 559. (c) Igersheim, F.; Mimoun, H. *Nouv. J. Chim.* **1980**, *4*, 161. (d) Drago, R. S.; Zuzich, A.; Nyberg, E. D. *J. Am. Chem. Soc.* **1985**, *107*, 2898. (e) Nyberg, E. D.; Pribitch, D. C.; Drago, R. S. *J. Am. Chem. Soc.* **1983**, *105*, 3538.

(12) Faraj, M.; Martin, J.; Martin, C.; Bregeault, J.-M. *J. Mol. Catal.* **1985**, *31*, 57.

(13) (a) Casado, M. A.; Pérez-Torrente, J. J.; López, J. A.; Ciriano, M. A.; Alonso, P. J.; Lahoz, F. J.; Oro, L. A. *Inorg. Chem.* **2001**, *40*, 4785. (b) Shaw, M. J.; Geiger, W. E.; Hyde, J.; White, C. *Organometallics* **1998**, *17*, 5486. (c) Carcia, M. P.; Jimenez, M. V.; Cuesta, A.; Siurana, C.; Oro, L. A.; Lahoz, F. J.; López, J. A.; Catalan, M. P.; Tiripicchio, A.; Lanfranchi, M. *Organometallics* **1993**, *12*, 3257. (d) For an example of a related, though less stable (N_3-ligand)Rh^{II}(diolefin) complex, see ref 16.

(14) Rossi, A. R.; Hoffmann, R. *Inorg. Chem.* **1975**, *14* (2), 365.

Downloaded by NAT LIB UKRAINE on July 6, 2009
Published on July 28, 2004 on http://pubs.acs.org | doi: 10.1021/om049654x

Table 1. Selected Bond Lengths (Å) for [1]$^+$, [2]$^{2+}$, and [5]$^{2+}$

	[**1**]$^+$	[**2**]$^{2+}$	[**5**]$^{2+}$
N1−Rh	2.2967(18)	2.068(7)	2.065(7)
N2−Rh	2.0859(19)	2.086(7)	2.050(7)
N3−Rh	2.2356(18)	2.021(6)	2.000(6)
C2−Rh	2.152(2)	2.069(8)	2.057(8)
C3−Rh	2.152(2)		
C5−Rh	2.066(2)		
C6−Rh	2.069(2)		
Cl−Rh		2.3799(18)	2.394(2)
Cl′−Rh		2.5945(18)	2.645(2)
C2−C3	1.380(3)	1.511(15)	1.637(15)
C5−C6	1.422(3)	*a*	*a*

[a] Bond length is unreliable because of very large anisotropic displacement.

Table 2. Selected Angles (deg) for [1]$^+$, [2]$^{2+}$ and [5]$^{2+}$

	[**1**]$^+$	[**2**]$^{2+}$	[**5**]$^{2+}$
N1−Rh−N2	93.07(7)	164.1(3)	165.3(3)
N1−Rh−N3	71.48(7)	82.2(3)	82.7(3)
N2−Rh−N3	78.61(7)	82.1(3)	82.9(3)
N1−Rh−C2	110.53(8)	87.4(4)	91.1(3)
N1−Rh−C3	86.68(8)		
N1−Rh−C5	120.10(8)		
N1−Rh−C6	159.69(8)		
N2−Rh−C2	152.46(8)	94.8(4)	92.9(3)
N2−Rh−C3	165.12(8)		
N2−Rh−C5	101.17(9)		
N2−Rh−C6	96.28(9)		
N3−Rh−C2	95.17(8)	88.0(3)	93.3(3)
N3−Rh−C3	115.21(8)		
N3−Rh−C5	168.32(8)		
N3−Rh−C6	128.08(8)		
C2−Rh−C3	37.39(9)		
C2−Rh−C5	79.60(9)		
C2−Rh−C6	66.31(9)		
C3−Rh−C5	66.50(10)		
C3−Rh−C6	79.68(9)		
C5−Rh−C6	40.24(9)		
N1−Rh−Cl		98.9(2)	99.1(2)
N1−Rh−Cl′		89.03(17)	87.73(19)
N2−Rh−Cl		96.4(2)	94.8(2)
N2−Rh−Cl′		88.47(17)	88.9(2)
N3−Rh−Cl		174.7(2)	173.4(2)
N3−Rh−Cl′		91.04(19)	89.1(2)
C2−Rh−Cl		97.2(3)	93.0(3)
C2−Rh−Cl′		176.4(3)	177.2(3)
Rh−Cl−Rh′		96.19(6)	95.35(7)
Cl−Rh−Cl′		83.81(6)	84.64(7)

indicate that N_{py} (N1) is a stronger σ-donor than N^H_{amine} (N3). Previously, however, we concluded that (for steric reasons) N^H_{amine} is a stronger σ-donor to Rh^I than N_{Py} in the related square pyramidal complex [(dpa)-Rh^I(cod)]$^+$ (dpa = *N*,*N*-di(2-pyridylmethyl)amine).[15a] The DFT-optimized geometries of [**1**]$^+$ and [(dpa)Rh^I(cod)]$^+$ are each very close to their X-ray structures. Apparently the difference in the relative donor strength of N_{Py} and N^H_{amine} is small, and the relative preference for these donors depends on the steric properties.

Oxidation of [(Me-dpa)Rh^I(nbd)]$^+$ to [(Me-dpa)-Rh^{II}(nbd)]$^{2+}$. Electrochemical oxidation of [**1**]$^+$ has been investigated by cyclic voltammetry in acetone and dichloromethane. In both solvents oxidation of [**1**]$^+$ to [**1**]$^{2+}$ proved reversible on the electrochemical time scale (acetone: $E_{1/2} = 0.113$ V, CH_2Cl_2: $E_{1/2} = 0.192$ V vs Fc/Fc$^+$). Irreversible oxidation of [**1**]$^{2+}$ is observed at higher potentials (acetone: $E > 1.144$ V, CH_2Cl_2: $E > 0.990$ V vs Fc/Fc$^+$ (for reasons of comparison these are *not* the peak potentials of the irreversible waves, but potentials at the feet of the wave where initial oxidation of [**1**]$^{2+}$ to [**1**]$^{3+}$ becomes measurable)).

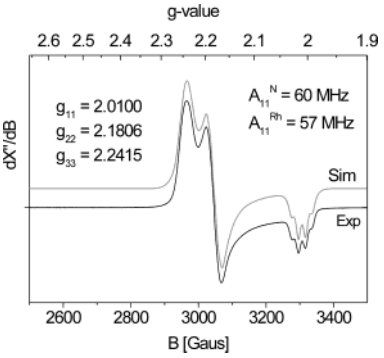

Figure 2. X-band EPR spectrum of [**1**]$^{2+}$ in frozen acetone at 20 K. Conditions: freq = 9.3014 GHz, mod. ampl. = 4 gauss, attenuation 30 dB. The simulation was obtained with the parameters included.

When the hexafluorophosphate salt of [**1**]$^+$ was dissolved in acetone and treated with silver hexafluorophosphate, a dark green solution was obtained. Treatment with diethyl ether yields a green precipitate of [**1**]$(PF_6)_2$. The EPR spectrum of [**1**]$^{2+}$ in frozen acetone at 20 K is shown in Figure 2.

Simulation of the rhombic spectrum yields $g_{11} = 2.0100$, $g_{22} = 2.1806$, and $g_{33} = 2.2415$. The signals at g_{22} and g_{33} are broadened, most probably by unresolved (super)hyperfine coupling with the rhodium and/or nitrogen nuclei ($A^{Rh} \leq 40$ MHz, $A^N \leq 40$ MHz). The resolved hyperfine coupling pattern for g_{11} was simulated by assuming a hyperfine coupling with rhodium, $A_{11}{}^{Rh} = 57$ MHz, and a superhyperfine coupling with one of the nitrogen nuclei, $A_{11}{}^N = 60$ MHz. Apart from the expected rhombicity, the EPR parameters of [**1**]$^{2+}$ are quite similar to those observed for the previously reported square pyramidal [(dpa)Rh^{II}(cod)]$^{2+}$, which has N^H_{amine} at the apical position.[16] This suggests that [**1**]$^{2+}$ is also square pyramidal, with the two nbd double bonds and the two inequivalent pyridine nitrogens coordinated in the basal plane (*x*,*y*) and the amine nitrogen at the apical position (*z*). Most likely, the SOMO of [**1**]$^{2+}$ consists predominantly of the rhodium d_{z^2} orbital with a small antibonding contribution from an orbital on N_{amine}. However, because the Rh^I complexes [**1**]$^+$ and

(15) The order of Lewis basicity of N-donor ligands to Rh^I(cod) (based on a correlation between ^{13}C NMR signals and redox potentials) was determined to be $N_{Hamine} > N_{Py} > N_{Py-Me}$. This seems to be of steric origin and parallels the known different orders of Brønsted and Lewis basicities of N-donors. Brønsted basicities of amines in the gas phase follow the inductive effect of the substituents at the nitrogen donor, but their Lewis basisity is mainly determined by steric factors. Order of Brønsted basicity of amines in the gas phase: $NH_3 < MeNH_2 < Me_2NH < NMe_3$. Order of Lewis basicity of amines toward BMe_3 in the gas phase: $NH_3 < NMe_3 < MeNH_2 < Me_2NH$ and $Et_3N < NH_3 < Et_2NH < EtNH_2$. Order of Lewis basicity of amines toward $B(CMe_3)_3$ in the gas phase: $Me_3N < Me_2NH < NH_3 < MeNH_2$ and $Et_3N < Et_2NH < EtNH_2 < NH_3$). For pyridine nitrogens, the orders of Lewis basicity and Brønsted basicity have been reported to be $N_{Py} > N_{Py-Me}$ and $N_{Py-Me} > N_{Py}$, respectively. (a) de Bruin, B.; Brands, J. A.; Donners, J. J. J. M.; Donners, M. P. J.; de Gelder, R.; Smits, J. M. M.; Gal, A. W.; Spek, A. L. *Chem. Eur. J.* **1999**, *5*, 2921. (b) Brown, H. C. *J. Am Chem. Soc.* **1945**, *67*, 378, 1452. (c) March, J. *Advanced Organic Chemistry*, 4th ed.; John Wiley & Sons: New York, 1992; pp 267 and 270. (d) Brown, H. C.; Bartholomay, H., Jr.; Taylor, M. D. *J. Am Chem. Soc.* **1944**, *66*, 435. (e) Cotton, F. A.; Wilkinson, G.; Gaus, P. L. *Basic Inorganic Chemistry*, 3rd ed.; John Wiley & Sons: New York, 1995; p 228.

(16) Hetterscheid, D. G. H.; de Bruin, B.; Smits, J. M. M.; Gal, A. W. *Organometallics* **2003**, *22*, 3022.

Downloaded by NAT LIB UKRAINE on July 6, 2009
Published on July 28, 2004 on http://pubs.acs.org | doi: 10.1021/om049654x

Scheme 2. Relative Energies (kcal/mol) of the Square Pyramidal Conformations of $[1]^{2+}$ (A, B, and C) and the Related dpa Complex $[(dpa)Rh^{II}(nbd)]^{2+}$ (D and E) as Obtained by DFT (b3-lyp level)[a]

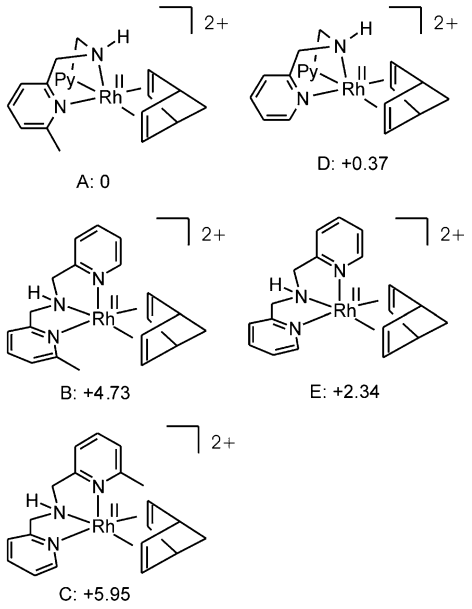

[a] For an easy comparison, the energy of the respective free N_3-ligand has been subtracted from the energy of each complex.

$[(dpa)Rh^{I}(cod)]^{+}$ choose to adopt different geometries in the crystal lattice, with another preference for the position of the N^{H}_{amine} donor, these similarity arguments are not conclusive. Therefore we performed some geometry optimizations of $[\mathbf{1}]^{2+}$ with DFT.

DFT Geometry Optimizations of $[(Me\text{-}dpa)Rh^{II}(nbd)]^{2+}$ and $[(dpa)Rh^{II}(nbd)]^{2+}$. Due to the Jahn−Teller effect, trigonal bipyramidal geometries of $[\mathbf{1}]^{2+}$ are not stable but immediately converge to square pyramidal geometries, invariably with the two double bonds of nbd in the basal plane. We optimized the DFT geometry of three such conformational local minima of $[\mathbf{1}]^{2+}$, each having a different N-donor of Me-dpa occupying the apical position (Scheme 2). The most stable geometry of $[\mathbf{1}]^{2+}$ is found to be square pyramid A with N3 (N^{H}_{amine}) at the apical position. The geometries B with N2 (N_{Py}) and C with N3 (N_{PyMe}) at the apical position are 4.73 and 5.95 kcal/mol higher in energy, respectively. The DFT SOMO of $[\mathbf{1}]^{2+}$ in conformation A mainly consists of the Rh d_{z^2} orbital with an antibonding contribution from an orbital on the N^{H}_{amine} donor. Thus, the DFT calculations support our conclusions from EPR.

According to Rossi and Hoffman, d^7 metals in a square pyramidal geometry have a tendency to form stronger basal σ-bonds than apical σ-bonds, although this tendency should be reduced compared to their d^8 analogues.[14] Indeed, as shown in Table 3, the calculated $Rh-N_{basal}$ bond distances of $[\mathbf{1}]^{2+}$ are shorter than the $Rh-N_{apical}$ bond distance in each of the conformations A, B, and C.

On the basis of previously reported bond strengths,[15] we must assume that (for steric reasons) the $Rh-N_{PyMe}$ bond is weaker than the $Rh-N_{Py}$ and $Rh-N_{Hamine}$ bonds. On the basis of the electronic arguments introduced by Rossi and Hoffman one would thus expect that conformation C should be preferred over B and A, because in this geometry the weakest $N_{PyMe}-Rh$ bond is formed at the preferred apical position (half-filled $d_{z^2}-N_{apical}$ antibonding character). Assuming that N_{Py} binds stronger to Rh(nbd) than N^{H}_{amine} (see X-ray structure of $[\mathbf{1}]^{+}$) in Me-dpa complexes, one would thus (based on electronic arguments only) predict the stability order C > A > B, whereas we calculate A > B > C.

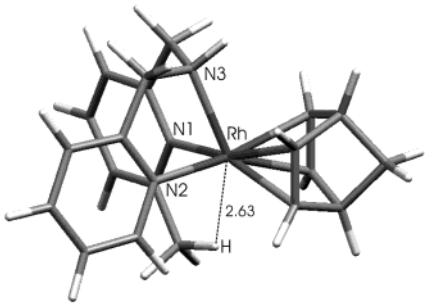

Figure 3. Stick drawing of the most stable conformation A of $[\mathbf{1}]^{2+}$ as obtained by DFT optimization. The dotted line represents an agostic interaction between a C−H bond of the MePy methyl group and the rhodium(II) center.

Table 3. Calculated (DFT) Rh−N and Rh−C Bond Lengths (Å) for $[\mathbf{1}]^{2+}$ in Conformations A, B, and C and $[(bpa)Rh^{II}(nbd)]^{2+}$ in Conformations D and E

	Rh−N3 (N_{amine})	Rh−N2 (N_{Py})	Rh−N1 (N_{MePy})
A	2.268[a]	2.115	2.135
B	2.146	2.225[a]	2.174
C	2.162	2.103	2.315[a]
D	2.259[a]	2.108, 2.109	
E	2.174	2.113, 2.222[a]	

[a] Apical position.

Repulsive interactions between the Me-dpa and nbd fragments must contribute to the higher energy of C and B compared to A. Furthermore, closer inspection of (the convergence to) the geometry of A reveals the presence of a stabilizing agostic interaction between a C−H bond of the MePy methyl group and the Rh^{II} center (Rh···H distance 2.63 Å). Although the respective C−H bond is not significantly elongated, this C−H fragment is clearly pointing toward the SOMO of A (see Figure 3).

To get a better feeling for the importance of steric contributions and the apparent agostic interaction, we compared the energies of Me-dpa complex $[\mathbf{1}]^{2+}$ in the conformations A, B, and C with those of the related hypothetical dpa complex $[(dpa)Rh^{II}(nbd)]^{2+}$ in conformations D and E (Scheme 2). The energies of D and E relative to A were calculated from $E_{(D/E)} = E^{tot}_{(D/E)} - E^{tot}_{(A)} - E^{tot}_{(dpa)} + E^{tot}_{(Medpa)}$.

Despite the fact that the $Rh-N_{MePy}$ interaction in $[\mathbf{1}]^{2+}$ is weaker than the $Rh-N_{Py}$ interaction in $[(dpa)Rh^{II}(nbd)]^{2+}$ (see Table 3), A is about 0.37 kcal/mol *more stable* than D. The complexes B and C (which lack any agostic interactions) are, respectively, 2.39 and 3.61 kcal/mol *less stable* than their dpa counterpart E. Increased steric repulsions between the methyl group of the PyMe donor and the nbd fragment in B and C compared to A will contribute to their higher energies, but computer-generated CPK models indicate that this is less important in B than in C. Therefore we can take the energy difference between B and E as a rough

Downloaded by NAT LIB UKRAINE on July 6, 2009
Published on July 28, 2004 on http://pubs.acs.org | doi: 10.1021/om049654x

Scheme 3. Oxidation of Rh^{I}(nbd) Complex $[1]^{+}$ to the Air-Stable Rh^{II}(nbd) Complex $[1]^{2+}$ [a]

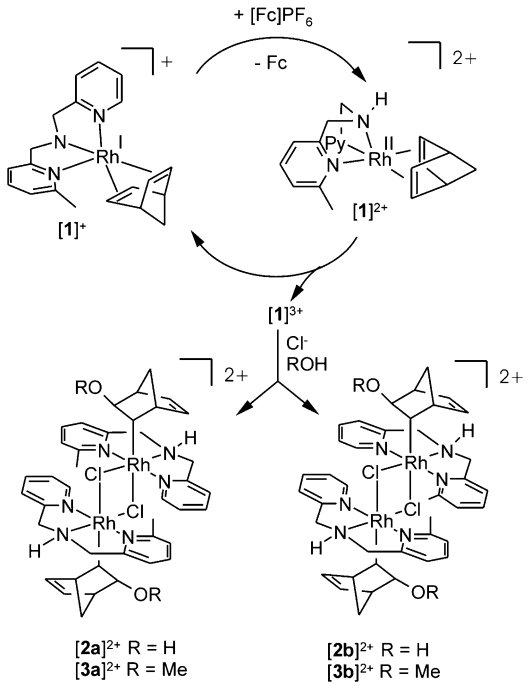

[a] Chloride ions trigger disproportionation of $[\mathbf{1}]^{2+}$ and formation of $[\mathbf{2a}]^{2+}$ and $[\mathbf{2b}]^{2+}$ in acetone/water or $[\mathbf{3a}]^{2+}$ and $[\mathbf{3b}]^{2+}$ in methanol.

indication for the destabilizing effect of replacing the basal N_{Py} donor in D by a basal N_{MePy} donor to obtain A. Accordingly, the stabilizing effect of the agostic interaction in A (which counter-effects this destabilization) should be about 2−3 kcal/mol. Although this is a weak interaction, it may indeed contribute to the preference of complex $[\mathbf{1}]^{2+}$ for conformation A.

Reaction of [(Me-dpa)Rh^{II}(nbd)]$^{2+}$ with Chloride and H_2O/MeOH. In contrast to $[(dpa)Rh^{II}(cod)]^{2+}$, nbd complex $[\mathbf{1}]^{2+}$ is stable in acetone at rt for 12−48 h. Although air accelerates its decomposition, $[\mathbf{1}]^{2+}$ is relatively air-stable in solution (30−60 min). $[(dpa)Rh^{II}(cod)]^{2+}$ spontaneously disproportionates to a 1:1 mixture of Rh^{I}(cod) and Rh^{III}(cycloocta-2,5-dien-1-yl)$]^{2+}$ at low temperatures, presumably via hydrogen abstraction from an allylic C−H bond of cod by the metalloradical M^{II} species.[16] Complex $[\mathbf{1}]^{2+}$ lacks a reactive allylic C−H bond, thus preventing such reactivity.

Remarkably, attempts to prepare $[\mathbf{1}]^{2+}$ by oxidation of $[\mathbf{1}]^{+}$ with equimolar amounts of $FeCl_3$ in an acetone/water mixture resulted in an entirely different reaction. Instead of the expected Rh^{II}(nbd) complex, the unique Rh^{III} η^1-3-hydroxynorbonenyl dinuclear complex $[\{(mer\text{-}\kappa^3\text{-Me-dpa})Rh^{III}(\eta^1\text{-3-hydroxynorborn-5-en-2-yl})(\mu_2\text{-Cl})\}_2](PF_6)_2$ ($[\mathbf{2}](PF_6)_2$) is obtained (Scheme 3). Due to the chirality of $[\mathbf{1}]^{+}$, the dinuclear complex $[\mathbf{2}]^{2+}$ is formed as a 1:1 mixture of the diastereomers $[\mathbf{2a}]^{2+}$ (meso, C_1 symmetric) and $[\mathbf{2b}]^{2+}$ (rac, C_2 symmetric).

Upon oxidation of [**1**]Cl with equimolar amounts of ferrocenium hexafluorophosphate ($[Fc]^{+}$ (PF_6^{-})) in MeOH a 2:1 mixture of diastereoisomers ($[\mathbf{3a}]^{2+}$ and $[\mathbf{3b}]^{2+}$) of $[\{(mer\text{-}\kappa^3\text{-Me-dpa})Rh^{III}(\eta^1\text{-3-methoxynorborn-5-en-2-yl})(\mu_2\text{-Cl})\}_2](PF_6)_2$ ($[\mathbf{3}](PF_6)_2$) precipitates from the solution (Scheme 3). Although the stoichiometric amounts of the oxidants $FeCl_3$ or $[Fc]^{+}$ were fully consumed in the above

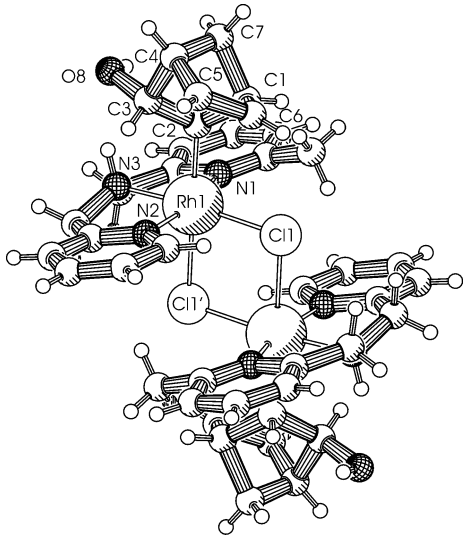

Figure 4. X-ray structure of $[\mathbf{2a}]^{2+}$.

reactions, approximately 50% of the starting material $[\mathbf{1}]^{+}$ was recovered as $[\mathbf{1}](PF_6)$, in agreement with the overall two-electron oxidation of Rh^{I} in $[\mathbf{1}]^{+}$ to Rh^{III} in $[\mathbf{2}]^{2+}$ and $[\mathbf{3}]^{2+}$. Higher yields of $[\mathbf{2}]^{2+}$ (70%) could be obtained by oxidizing $[\mathbf{1}]^{+}$ with an excess of $FeCl_3$. Similar attempts to obtain higher yields of $[\mathbf{3}]^{2+}$ by using an excess of $[Fc]^{+}$ however did not significantly improve the yield of this reaction (max. obtained yield of 17% upon oxidation with 2 equiv of $[Fc]^{+}$). The remainder is a gray insoluble material, which we were unable to characterize.

Obviously, the complexes $[\mathbf{2}]^{2+}$ and $[\mathbf{3}]^{2+}$ result from nucleophilic attack of respectively OH^{-} from water and MeO^{-} from methanol. Due to the associated release of H^{+}, besides formation of $[\mathbf{2}]^{2+}$ or $[\mathbf{3}]^{2+}$ two diastereoisomeric forms of a new complex ($[\mathbf{5}]^{2+}$) were obtained in low yields (∼5%). These complexes ($[\mathbf{5a}]^{2+}$ and $[\mathbf{5b}]^{2+}$) show ^{1}H NMR signals quite similar to those of $[\mathbf{2}]^{2+}$ and $[\mathbf{3}]^{2+}$, but are actually formed by protonation of $[\mathbf{1}]^{+}$ (vide infra).

Crystals of $[\mathbf{2}](BPh_4)_2$ suitable for X-ray diffraction were obtained by crystallization from acetone/dioxane in the presence of tetraphenylborate. The X-ray structure of $[\mathbf{2a}]^{2+}$ is shown in Figure 4. Selected bond lengths and angles are summarized in Tables 1 and 2. Unfortunately, the crystals obtained are actually cocrystals of $[\mathbf{2a}]^{2+}$ and $[\mathbf{2b}]^{2+}$, in which $[\mathbf{2a}]^{2+}$ prevails. This causes some disorder, which could not be adequately resolved. Nevertheless, the molecular structure of $[\mathbf{2}]^{2+}$ is clear from the X-ray structure determination. The norbornenyl fragments of $[\mathbf{2}]^{2+}$ are both η^1-coordinated via only one rhodium−carbon bond and contain a noncoordinated double bond. The other double bond of nbd has undergone *exo* attack of a hydroxide, and thus the resulting C−O bond is in *trans* position to the rhodium−carbon bond. The ligand is bound in a meridional way. The change of the coordination mode of Me-dpa from *fac* to *mer* is probably caused by the strong *trans* effect of the carbon coordinated to rhodium. Two equivalent chloride ions bridge between the two rhodium(III) centers on the positions *trans* with respect to the norbornadienyl and the N_{amine} positions. As a result, the double bond of the norbornadiene fragment is no longer coordinated to rhodium.

Downloaded by NAT LIB UKRAINE on July 6, 2009
Published on July 28, 2004 on http://pubs.acs.org | doi: 10.1021/om049654x

Downloaded by NAT LIB UKRAINE on July 6, 2009
Published on July 28, 2004 on http://pubs.acs.org | doi: 10.1021/om049654x

Oxidation of $[\mathbf{1}]^+$ to $[\mathbf{1}]^{2+}$ proved reversible on the electrochemical time scale of our cyclic voltammetry (CV) measurements (100 mV/s). However, addition of chloride to the solution yields a completely irreversible oxidation wave in CV. Also upon addition of water, oxidation of $[\mathbf{1}]^+$ to $[\mathbf{1}]^{2+}$ becomes irreversible in CV. Indeed, addition of water to isolated $[\mathbf{1}]^{2+}(PF_6)_2$ causes rapid decomposition of the Rh^{II}(nbd) complex to an unidentified mixture of compounds. However, in the absence of Cl^- this reaction does not result in an analogue of $[\mathbf{2}]^{2+}$. Addition of methanol does not influence the voltammogram of $[\mathbf{1}]^+$. These observations indicate that formation of $[\mathbf{2}]^{2+}$ and $[\mathbf{3}]^{2+}$ is triggered by chloride, most likely via a disproportionation reaction (Scheme 3). Unassisted disproportionation of $[\mathbf{1}]^{2+}$ to $[\mathbf{1}]^+$ and $[\mathbf{1}]^{3+}$ in acetone is highly unfavorable ($\Delta G° >$ 23 kcal/mol, estimated from the $E_{1/2}$ value for the $[\mathbf{1}]^+/[\mathbf{1}]^{2+}$ couple and the potential at which initial oxidation of $[\mathbf{1}]^{2+}$ to $[\mathbf{1}]^{3+}$ becomes measurable at the feet of the corresponding irreversible wave in CV). According to our CV measurements, disproportionation in CH_2Cl_2 is still unfavorable, but significantly less endothermic ($\Delta G° >$ 18 kcal/mol) than in acetone. A rapid follow-up reaction (e.g., Cl^- abstraction) of $[\mathbf{1}]^{3+}$ with CH_2Cl_2 might be responsible for this difference. In the presence of Cl^- disproportionation of $[\mathbf{1}]^{2+}$ may become more favorable or even exothermic by formation of Cl^- adducts of $[\mathbf{1}]^{2+}$ and $[\mathbf{1}]^{3+}$. The resulting dicationic Cl^- adduct of $[\mathbf{1}]^{3+}$ is still likely to undergo nucleophilic attack of water or methanol (Scheme 3).

An alternative mechanism in which homolytic bond splitting of the water or methanol O−H bond occurs between two Rh^{II} sites is unlikely, although such reactions have been proposed to occur in the reaction of low-spin cobalt(II) species with H_2O.[17] In the present case, this would have resulted in *endo* attack instead of the observed *exo* attack.

Protonation of Rh^{I}(nbd). Due to experimental restrictions, formation of $[\mathbf{2}]^{2+}$ must be performed in protic media. Since we expected that protonation of $[\mathbf{1}]^+$ plays a role in the associated formation of $[\mathbf{5}]^{2+}$, we decided to investigate the reactivity of $[\mathbf{1}]^+$ toward a variety of acids.

In the absence of Cl^-, irrespective of the acid used, protonation of $[\mathbf{1}]^+$ mainly occurs at a pyridine group of the Me-dpa ligand, yielding the corresponding square planar complex $[(\kappa^2\text{-Me-dpa}H)Rh^{I}(nbd)]^{2+}$ ($[\mathbf{4}]^{2+}$, Scheme 4). Protonation of $[\mathbf{1}]^+$ results in broad ^1H NMR spectra at rt, indicative of formation of several complexes in equilibrium. These spectra are quite similar to those obtained after protonation of $[(dpa)Rh^{I}(cod)]^+$.[15,16] In the absence of Cl^-, $[\mathbf{4}]^{2+}$ is stable, but the presence of Cl^- triggers migration of H^+ from the MedpaH^+ ligand to a double bond of nbd. This results in the η^1-norborn-5-en-2-yl dinuclear complex $[\{(mer\text{-}\kappa^3\text{-Me-dpa})Rh^{III}(\eta^1\text{-norborn-5-en-2-yl})(\mu_2\text{-Cl})\}_2]^{2+}$ ($[\mathbf{5}]^{2+}$) (Scheme 4). Dinuclear complex $[\mathbf{5}]^{2+}$ precipitates from MeOH as a 1:1 mixture of the diastereomers $[\mathbf{5a}]^{2+}$ (meso, C_1 symmetric) and $[\mathbf{5b}]^{2+}$ (rac, C_2 symmetric). Besides $[\mathbf{5a}]^{2+}/[\mathbf{5b}]^{2+}$ (72%), protonation of $[\mathbf{1}]^+$ with HCl yields several impurities.

Crystals of $[\mathbf{5}](PF_6)_2$ suitable for X-ray diffraction were obtained by crystallization from acetone/dioxane. The X-ray structure of $[\mathbf{5}]^{2+}$ is shown in Figure 5. Unfortunately, as in $[\mathbf{2a}]^{2+}/[\mathbf{2b}]^{2+}$, the crystals obtained are actually nearly 1:1 cocrystals of $[\mathbf{5a}]^{2+}$ and $[\mathbf{5b}]^{2+}$. This causes some disorder, which could not be entirely resolved.

The structure of $[\mathbf{5}]^{2+}$ is similar to the structure of $[\mathbf{2}]^{2+}$ with the Me-dpa ligand bound in a meridional way. The η^1-norbornenyl fragment is coordinated via only one rhodium−carbon bond and contains a noncoordinated double bond. Two equivalent chloride ions bridge between two rhodium centers.

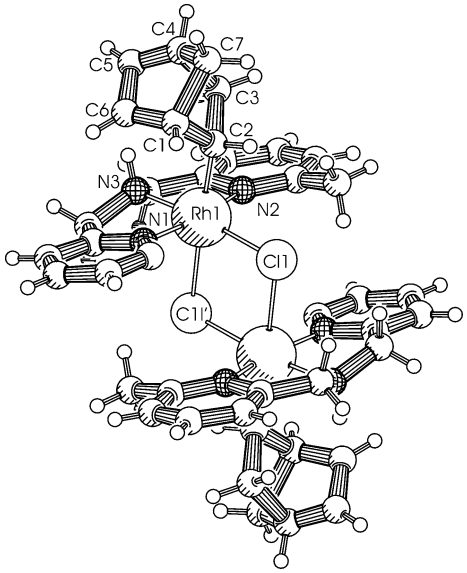

Figure 5. X-ray structure of $[\mathbf{5a}]^{2+}$.

Scheme 4. Protonation of $[\mathbf{1}]^+$ to Give $[\mathbf{4}]^{2+}$ [a]

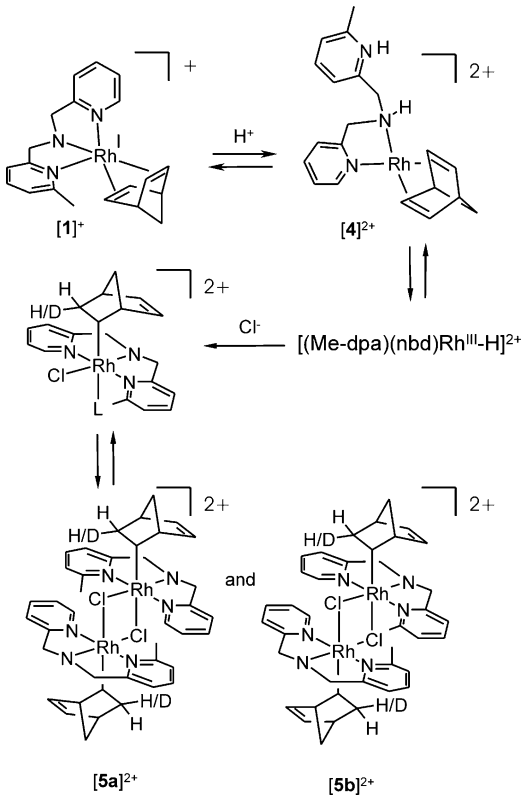

[a] Chloride ions trigger migration of the proton from the pyridine fragment in $[\mathbf{4}]^{2+}$ to the nbd fragments in $[\mathbf{5a}]^{2+}$ and $[\mathbf{5b}]^{2+}$.

(17) Griffith, W. P.; Wilkinson, G. *J. Chem. Soc.* **1959**, 2757.

Downloaded by NAT LIB UKRAINE on July 6, 2009
Published on July 28, 2004 on http://pubs.acs.org | doi: 10.1021/om049654x

Preparation of $[\mathbf{5}]^{2+}$ by protonation of [**1**]Cl with D_2SO_4 yields a ^1H NMR spectrum from which the signal of the proton *cis* to rhodium has disappeared. This indicates that protonation of the olefinic double bond must have occurred via the rhodium center.

Apparently, Cl^- triggers migration of H^+ from Me-dpaH^+ to the metal. A coordinated double bond of nbd inserts in the thus obtained $Rh^{III}-H$ bond, forming a norborn-5-en-2-yl complex. The strong *trans* influence of the obtained alkyl fragment probably induces *mer* coordination of Me-dpa and η^1-coordination of the norborn-5-en-2-yl fragment. The observed *endo* attack of H^+ contrasts the *exo* attack of OH^- in the oxidation reaction of $[\mathbf{1}]^+$ to $[\mathbf{2}]^{2+}$ described above and the results of Speckman et al.[18] In this last case protonation of [*closo*-3,3-(η^4-bicylco[2.2.1]hepta-2,5-diene)-1,2-$(CH_3)_2$-3,1,2-$RhC_2B_9H_9]^-$ resulted in *exo* attack of H^+ by direct protonation of a nbd double bond. For protonated [*closo*-3,3-(η^4-bicylco[2.2.1]hepta-2,5-diene)-1,2-$(CH_3)_2$-3,1,2-$RhC_2B_9H_9]^-$ rearrangement of norborenyl to ethylcyclopentadienyl was observed. Such rearrangement was not observed for $[\mathbf{5}]^{2+}$, which is stable in solution.

For both $[\mathbf{5a}]^{2+}$ and $[\mathbf{5b}]^{2+}$, the proton at the metal-bound C2 carbon appears at a remarkably downfield ^1H NMR chemical shift of 5.1 ppm, whereas one would expect a much more upfield shift (1−3 ppm). Assignment of this signal was confirmed by NOESY spectroscopy. Anisotropic deshielding by the pyridine groups may cause this downfield shift. The same shifts are observed for the proton on C2 of $[\mathbf{2}]^{2+}$ and $[\mathbf{3}]^{2+}$.

The ^1H NMR signals of $[\mathbf{5}]^{2+}$ are slightly broadened, and clear exchange signals between characteristic signals for $[\mathbf{5a}]^{2+}$ and $[\mathbf{5b}]^{2+}$ were observed in the NOESY/EXSY spectrum. Similar line broadening of the ^1H NMR signals of $[\mathbf{2}]^{2+}$ and $[\mathbf{3}]^{2+}$ indicated that in all three cases the observed diastereoisomers are in equilibrium with each other at the NMR time scale. The dimeric complexes are probably in equilibrium with their monomers, which must be present in very low concentrations. Apparently, the rhodium−chloride bond is easily and reversibly broken as a result of the *trans* effect of the rhodium−carbon bond. This was confirmed by addition of coordinating reagents. Dissolving $[\mathbf{5}]^{2+}$ in coordinating solvents such as DMF splits the chloride bridges and results in the mononuclear solvate [{(*mer*-κ^3-Me-dpa)-Rh^{III}(η^1-norborn-5-en-2-yl)(Cl)(DMF)}]$^+$. The pyridine-H5 signals of $[\mathbf{5}]^{2+}$ in acetone occur at 7.2−7.0 ppm in ^1H NMR due to anisotropic shielding by other pyridine groups, as a result of the close proximity of the two Me-dpa ligands in this dinuclear complex. In the ^1H NMR spectra of the mononuclear DMF adduct of $[\mathbf{5}]^{2+}$ these signals occur in a normal region (>7.4 ppm). For $[\mathbf{2}]^{2+}$ and $[\mathbf{3}]^{2+}$ similar mononuclear complexes are obtained upon treatment with DMF (^1H NMR), but NMR indicates formation of a more complex mixture in these cases. This is probably due to formation of isomeric mixtures (due to exchange of Cl^- and DMF positions), since ESI-MS indicates mass-identical species.

Elimination of Norbornenone from Rh^{III}(η^1-3-hydroxynorbornenyl). The structure of the η^1-3-hydroxynorbornenyl rhodium complex $[\mathbf{2}]^{2+}$ is unique. Nucleophilic attack to other M(diolefin) complexes (M = Pd^{II}, Rh^{III}, Ir^{III}) has invariably resulted in η^3-coordinated norbornenyl derivatives.[5−9] In contrast to the observed behavior of related η^3-norbornenyl complexes, the unusual η^1-coordination mode of the 3-hydroxynorbornenyl fragment in $[\mathbf{2}]^{2+}$ suggests that it should be possible to eliminate norbornenone. Elimination of norbornenone from $[\mathbf{2}]^{2+}$ is indeed observed, although this is not a very easy process. Addition of silver salts to abstract the chloro ligands or refluxing in acetone/water mixtures failed to induce norbornenone elimination. Thermolysis of $[\mathbf{2}]^{2+}$ by heating the compound for 6 h at 100 °C in DMF however results in nearly quantitative formation of norbornenone (as observed with GC, GC−MS, and ^1H NMR). Besides norbornenone a complex mixture of rhodium compounds was formed. If the same experiment is conducted in the presence of an excess of norbornadiene, about 60% (based on ^1H NMR integration) of the rhodium material is recovered as the starting material $[\mathbf{1}]^+$. The elimination of norbornenone from $[\mathbf{2}]^{2+}$ most likely proceeds via β-hydrogen elimination. Deprotonation of the resulting Rh^{III}-H species in the presence of nbd then gives Rh^I(nbd). In an attempt to make these stoichiometric reactions catalytic (Scheme 5), oxidation of $[\mathbf{1}]^+$ by $FeCl_3$ in the presence of norbornadiene was carried out at 100 °C in DMF. However, so far we failed to observe more than 1−2 turnovers. Nevertheless, the reaction sequence involving oxidation of $[\mathbf{1}]^+$ to $[\mathbf{2}]^{2+}$ followed by decomposition of $[\mathbf{2}]^{2+}$ to $[\mathbf{1}]^+$ and norbornenone in the presence of nbd in principle provides a route to the desirable Wacker type oxidation of norbornadiene to norbornenone.

Scheme 5. Possibilities for Catalytic Oxidation of Norbornadiene to Norbornenone

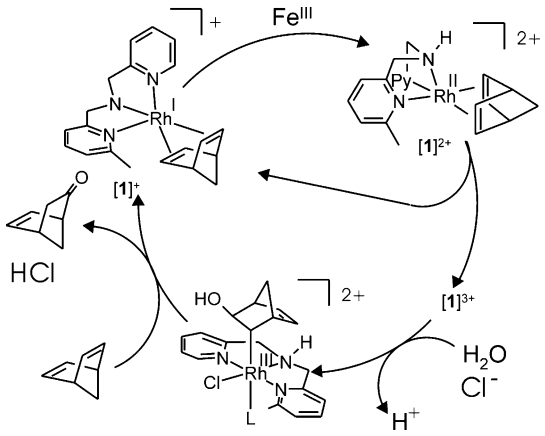

Concluding Remarks

Single-electron oxidation of [(Me-dpa)Rh^I(nbd)]$^+$ results in the relatively (air) stable [(Me-dpa)Rh^{II}(nbd)]$^{2+}$, which is a rare example of a isolated and fully characterized rhodium(II)-olefin species. Disproportionation of this Rh^{II} species is induced by the presence of Cl^- and yields [(Me-dpa)Rh^{III}(nbd)]$^{3+}$ or its Cl^- adduct. The resulting electrophilic Rh^{III} species undergo nucleophilic attack at the coordinated nbd fragment to yield η^1-coordinated norbornenyl complexes. Relevant to Wacker type oxidations at rhodium, the stereochemistry of the obtained unique Rh^{III}(η^1-norbornenyl) fragments reveals that nucleophilic attack of OH^- or MeO^- occurs directly

(18) Speckman, D. M.; Knobler, C. B.; Hawthorne, M. F. *Organometallics* **1985**, *4*, 1692.

at the nbd fragment, whereas electrophilic addition of $H^+(D^+)$ to $[(Me\text{-}dpa)Rh^I(nbd)]^+$ initially occurs at the N-ligand. The presence of Cl^- triggers migration of H^+ from the MedpaH^+ ligand to a double bond of nbd via the rhodium center.

The possibility of *fac* to *mer* rearrangement of the podal Me-dpa may well be important in order to obtain the novel η^1-hydroxynorbornenyl complexes. In contrast to related η^3-3-hydroxynorbornenyl palladium complexes, this η^1-coordination mode allows elimination of norbornenone upon heating. Although we can only present about one turnover at this point, the reaction sequences presented in this paper in principle provide a catalytic cycle for the desirable Wacker type oxidation of norbornadiene to norbornenone. Using this strategy for other metals or olefins might lead to future development of new Wacker type catalysts for specific monooxygenation of norbornadiene and other diolefinic substrates.

Downloaded by NAT LIB UKRAINE on July 6, 2009
Published on July 28, 2004 on http://pubs.acs.org | doi: 10.1021/om049654x

Experimental Section

General Procedures. All procedures were performed under N_2 with standard Schlenk techniques unless indicated otherwise. Solvents (p.a.) were deoxygenated by bubbling through a stream of N_2 or by freeze−pump−thaw method. The temperature indication room temperature (rt) corresponds to about 20 °C. NMR experiments were carried out on a Bruker DPX200 (200 and 50 MHz for ^1H and ^{13}C, respectively), a Bruker AC300 (300 and 75 MHz for ^1H and ^{13}C, respectively), and a Bruker AM500 (500 and 125 MHz for ^1H and ^{13}C, respectively). Solvent shift reference for ^1H spectroscopy: [D_6]-acetone $\delta_H = 2.05$, $CDCl_3$ $\delta_H = 7.28$, [D_6]dimethylformamide $\delta_H = 2.74$. For ^{13}C NMR: [D_6]acetone $\delta_C = 29.5$, $CDCl_3$ $\delta_C = 77.0$, [D_6]dimethylformamide $\delta_C = 30.11$. Abbreviations used are s = singlet, d = doublet, dd = doublet or doublets, t = triplet, m = multiplet, br = broad. Elemental analyses (CHN) were carried out by the Analytische Laboratorien in Lindlar (Germany). Cyclic voltammetry measurements were performed with an Eco Chemie Autolab PGSTAT20. A conventional three-electrode cell, with Pt working and auxiliary electrodes and 0.1 M $[(Bu)_4N]PF_6$ (TBAH) electrolyte, was used. An Ag/AgI reference electrode (grain of AgI, 0.02 M $[(Bu)_4N]I$ (TBAI) and 0.1 M TBAH) was employed. Experimental X-band EPR spectra were recorded on a Bruker ER220 spectrometer. The spectra were simulated by iteration of the anistropic *g* values, (super)hyperfine coupling constants, and line widths. We thank Dr. F. Neese (Bioanorganische Chemie, Mülheim a/d Ruhr, Germany) for a copy of his EPR simulation program. The complex $[Rh(nbd)Cl]_2$ was prepared according to literature procedures.[19] All other chemicals are commercially available and were used without further purification, unless stated otherwise.

X-ray Diffraction. The structures of $[\mathbf{1}]^+$, $[\mathbf{2}]^{2+}$, and $[\mathbf{5}]^{2+}$ are shown in Figures 1, 4, and 5, respectively. Drawings were generated with the program PLATON.[20] Selected bond distances and angles are given in Tables 1 and 2. Other relevant structure data are summarized in Table 4. The structures were solved by the program system DIRDIF[21] using the program PATTY[22] to locate the heavy atoms. All non-hydrogen atoms were refined with standard methods (refinement against F^2 of all reflections with SHELXL-97[23]) with anisotropic parameters for the non-hydrogen atoms. The hydrogen atoms were placed at calculated positions and refined isotropically in riding mode.

$[\mathbf{1}]^+(PF_6)$. The PF_6 moiety is rather disordered. It was attempted to describe this disorder, but the result is not very satisfactory and should be used carefully. Geometrical calculations[20] revealed neither unusual geometric features nor unusual short intermolecular contacts. The calculations revealed no higher symmetry and no (further) solvent accessible areas.

$[\mathbf{2}]^{2+}(BPh_4)_2$. It proved to be impossible to grow good quality crystals, which is reflected in the results of the crystal structure determination. The structure shows considerable disorder, which could not be described adequately; efforts to do so resulted in unstable refinements. The substituted norbornadiene fragment (C1−C7, O8) shows very large anisotropic displacement parameters, and bond distances and angles should be treated as being unreliable. The atomic type assignment of O8 and the unsaturated double bond type assignment to C5−C6 are based solely on chemical and spectroscopic evidence and are not supported by crystallographic data.

Also the BPh_4^- moiety shows some unacceptably large anisotropic displacement parameters, but that is no reason not to trust its nature or its presence in the structure. Trials to solve the structure in P1 were not successful. It even proved to be impossible to find the complete set of atomic parameters from the available data.

Geometrical calculations[20] revealed no further unusual geometric features or unusual short intermolecular contacts. The calculations revealed no higher symmetry and no (further) solvent accessible areas.

$[\mathbf{5}]^{2+}(PF_6)_2$. Only one methylpyridine is present in the complex but the methyl was found to be disordered over two positions, C17 and C27, with occupation factors of 0.57 and 0.43, respectively. Besides that the structure shows some more disorder, which could not be described adequately, resulting in some rather large thermal displacement parameters. Some unidentified, disordered, and only partially occupied solvent molecules were found. This electron density was accounted for by applying the SQUEEZE procedure,[20] which showed a void of 126 Å^3 containing 10 electrons. Geometrical calculations[20] revealed neither unusual geometric features nor unusual short intermolecular contacts. The calculations revealed no higher symmetry and no (further) solvent accessible areas.

Crystallographic data (excluding structure factors) for the structures reported in this paper have been deposited with the Cambridge Crystallographic Data Centre as supplementary publication no. CCDC 235598 for $[\mathbf{1}]PF_6$, 23599 for $[\mathbf{2}](BPh_4)_2$, and 235600 for $[\mathbf{5}](PF_6)_2$. Copies of available material can be obtained, free of charge, on application to the Director, CCDC, 12 Union Road, Cambridge CB2 1EZ, UK (fax: +44-(0) 1223-336033 or e-mail: teched@chemcrys.cam.ac.uk).

(19) (a) Chatt, J.; Venanzi, J. *J. Chem. Soc.* **1957**, 4735. (b) Abel, E. W.; Bennett, M. A.; Wilkinson, G. *J. Chem. Soc.* **1959**, 3178. (c) Schrock, R. R. *J. Am. Chem. Soc.* **1971**, *93*, 2397.

(20) Spek, A. L. *PLATON*, A Multipurpose Crystallographic Tool; Utrecht University: Utrecht, The Netherlands, 2003.

(21) Beurskens, P. T.; Beurskens, G.; Bosman, W. P.; de Gelder, R.; García-Granda, S.; Gould, R. O.; Israël, R.; Smits, J. M. M. *DIRDIF-96*, A computer program system for crystal structure determination by Patterson methods and direct methods applied to difference structure factors; Laboratory of Crystallography, Department of Inorganic Chemistry, University of Nijmegen: The Netherlands, 1996.

(22) Beurskens, P. T.; Beurskens, G.; Strumpel, M.; Nordman, C. E. In *Patterson and Pattersons*; Glusker, J. P., Patterson, B. K., Rossi, M., Eds.; Clarendon Press: Oxford, 1987; p 356.

(23) Sheldrick, G. M. *SHELXL-97*, Program for the refinement of crystal structures; University of Göttingen: Germany, 1997.

(24) (a) Ahlrichs, R.; Bär, M.; Baron, H.-P.; Bauernschmitt, R.; Böcker, S.; Ehrig, M.; Eichkorn, K.; Elliott, S.; Furche, F.; Haase, F.; Häser, M.; Hättig, C.; Horn, H.; Huber, C.; Huniar, U.; Kattannek, M.; Köhn, A.; Kölmel, C.; Kollwitz, M.; May, K.; Ochsenfeld, C.; Öhm, H.; Schäfer, A.; Schneider, U.; Treutler, O.; Tsereteli, K.; Unterreiner, B.; von Arnim, M.; Weigend, F.; Weis, P.; Weiss, H. *Turbomole Version 5*; Theoretical Chemistry Group, University of Karlsruhe, 2002. (b) Treutler, O.; Ahlrichs, R. *J. Chem. Phys.* **1995**, *102*, 346. (c) Turbomole basis set library: *Turbomole* Version 5, see ref 20a. (d) Schäfer, A.; Horn, H.; Ahlrichs, R. *J. Chem. Phys.* **1992**, *97*, 2571. (e) Andrae, D.; Haeussermann, U.; Dolg, M.; Stoll, H.; Preuss, H. *Theor. Chim. Acta* **1990**, *77*, 123. (f) Schäfer, A.; Huber, C.; Ahlrichs, R. *J. Chem. Phys.* **1994**, *100*, 5829.

Table 4. Crystallographic Data for [1]PF_6, [2]$(BPh_4)_2$, and [5]$(PF_6)_2$

	[**1**]PF_6	[**2**]$(BPh_4)_2$	[**5**]$(PF_6)_2$
empirical formula	$C_{20}H_{23}F_6N_3PRh$	$C_{68}H_{64}B_2Cl_2N_6O_2Rh_2$	$C_{40}H_{46}Cl_2F_{12}N_6P_2Rh_2$
cryst color	transparent yellow	transparent yellow brown	transparent light brown yellow
cryst shape	rough fragment	rough fragment	rough rod
cryst size (mm)	0.22 × 0.20 × 0.18	0.27 × 0.21 × 0.08	0.21 × 0.06 × 0.05
molecular weight	553.29	1559.98	1177.48
T (K)	208(2)	208(2)	208(2)
cryst syst	monoclinic	triclinic	monoclinic
space group	$P2_1/n$	$P\bar{1}$	$C2/c$
volume (Å^3)	2118.0(6)	1848.84(17)	4795(2)
a (Å)	10.8225(12)	10.2395(5)	13.173(3)
b (Å)	13.335(2)	13.8332(7)	22.340(6)
c (Å)	14.711(3)	14.5277(8)	16.478(4)
α (deg)	90	68.189(4)	90
β (deg)	93.947(12)	86.382(5)	98.61(2)
γ (deg)	90	75.528(4)	90
$\rho_{calcd.}$ (g·cm^{-3})	1.735	1.401	1.631
Z	4	1	4
diffractometer	Nonius KappaCCD	Nonius KappaCCD	Nonius KappaCCD
abs coeff (mm^{-1})	0.947	0.573	0.949
scan	area detector ϕ and ω scan	area detector ϕ and ω scan	area detector ϕ and ω scan
radiation (graphite mon.)	Mo Kα	Mo Kα	Mo Kα
wavelength (Å)	0.71073	0.71073	0.71073
F(000)	1112	808	2360
θ range [deg]	4.53−27.53	3.54−22.50	3.10−22.50
index ranges h	−14 ≤ 14	−11 ≤ 11	−14 ≤ 14
k	−17 ≤ 17	−14 ≤ 14	−24 ≤ 24
l	−19 ≤ 19	−15 ≤ 15	−17 ≤ 17
abs corr	SADABS multiscan correction[a]	SADABS multiscan correction[a]	SADABS multiscan correction[a]
no. of measd reflns	62 793	27 741	32 568
no. of unique reflns	4850	4822	3127
R_{int}	0.0531	0.0528	0.0993
no. of obsd reflns [$I_0 > 2\sigma(I_0)$]	3947	3681	2540
no. of data/restrains/params	4850/0/341	4822/0/462	3127/0/296
goodness-of-fit on F^2	1.023	1.041	1.083
SHELXL-97 weight params	0.0272, 1.5373	0.0838, 4.9384	0.0613, 47.0625
final R1, wR2 [$I > 2\sigma(I)$]	0.0265, 0.0576	0.0653, 0.1577	0.0620, 0.1377
R1, wR2 (all data)	0.0388, 0.0612	0.0902, 0.1738	0.0816, 0.1473
diff peak and hole (e· Å^{-3})	0.475, −0.430	1.178, −0.403	0.599, −0.422

[a] Sheldrick, G. M. *SADABS*, Program for Empirical Absorption Correction; University of Göttingen: Germany, 1996.

Downloaded by NAT LIB UKRAINE on July 6, 2009
Published on July 28, 2004 on http://pubs.acs.org | doi: 10.1021/om049654x

DFT Calculations. All calculations were carried out with the Turbomole program[24a] coupled to the PQS Baker optimizer.[25] Geometries were fully optimized as minima at the bp86[26] level using the Turbomole SV(P) basis set[24c,d] on all atoms (small-core pseudopotential[24c,e] on Rh). Improved energies were obtained from single-point calculations at the b3-lyp level[27] using the TZVP basis[24c,f] (small-core pseudopotential[24c,e] on Rh).

Synthesis of *N*-(2-Pyridylmethyl)-*N*-(6-methyl-2-pyridylmethyl)amine (Me-dpa). To a solution of 5.5 g of 2-pyridylmethylamine in 50 mL of MeOH was added 6.0 g of 6-methyl-2-pyridylmethylcarboxaldehyde. The solution was stirred for 1 h, after which 1.5 g of $NaBH_4$ was added at 0 °C. The solution was again stirred for 1 h at room temperature. Concentrated hydrochloric acid was added and the solvent partly evaporated. To the reaction mixture were added 40 mL of demineralized water and Na_2CO_3. The solution was washed with 3 × 20 mL of dichloromethane. The combined organic layers were dried and concentrated in vacuo, yielding a dark yellow oil of crude Me-dpa, which was directly used for further reactions. ^{1}H NMR (200 MHz, $CDCl_3$, 298 K): δ 8.54 (d, $^3J_{H,H}$ = 3.24, 1H, Py *H*6), 7.63 (dt, $^3J_{H,H}$ = 5.12 Hz, $^4J_{H,H}$ =1.35 Hz, 1H, Py *H*4), 7.51 (t, $^3J_{H,H}$ = 5.12 Hz, PyMe *H*4), 7.35 (d, $^3J_{H,H}$ = 5.12 Hz, 1H, Py *H*3), 7.1−7.12 (m, 2H, Py *H*5 en PyMe *H*3), 7.00 (d, $^3J_{H,H}$ = 5.12 Hz, PyMe *H*5), 3.98 (s, 2H, CH_2), 3.94 (s, 2H, CH_2), 3.11 (s, 1H, N*H*), 2.52 (s, 3H, Py*Me*). ^{13}C NMR (50 MHz, $CDCl_3$, 298 K): δ 159.9 (Py *C*2 or PyMe *C*2), 159.0 (Py *C*2 or PyMe *C*2), 157.8 (PyMe *C*6), 149.2 (Py *C*6), 136.6 (Py *C*4 or PyMe *C*4), 136.4 (Py *C*4 or PyMe *C*4), 122.2 (Py *C*3, PyMe *C*3 or Py *C*5), 121.9 (Py *C*3, PyMe *C*3 or Py *C*5), 121.4 (Py *C*3, PyMe *C*3, or Py *C*5), 119.1 (PyMe *C*5), 54.9, 54.2 (*C*H_2), 24.5 (Py*Me*).

Synthesis of [(η^4-Norborna-1,4-diene)-(κ^3-fac-*N*-(2-pyridylmethyl)-*N*-(6-methyl-2-pyridylmethyl)amine)rhodium(I)] Chloride/Hexafluorophosphate ([1]Cl/[1]PF_6). [Rh(nbd)Cl] (2.8 g) was stirred in 10 mL of methanol. To the suspension Me-dpa was added dropwise until a bright orange solution of [**1**]Cl was obtained. Treatment with an excess of NH_4PF_6 caused precipitation of [**1**]PF_6 as a yellow powder (3.1 g/50%). The solid was washed with methanol and dried in vacuo. Recrystallization from acetone/dioxane yields crystals, which were used for X-ray diffraction. ^{1}H NMR (300 MHz, [D_6]acetone, 298 K): δ 8.05 (d, $^3J_{H,H}$ = 5.7 Hz, 1H, Py *H*6), 7.74 (m, 1H, Py *H*4), 7.68 (t, $^3J_{H,H}$ = 7.7 Hz, 1H, MePy *H*4), 7.38−7.19 (m, 4H, Py *H*3, Py *H*5, MePy *H*3, MePy *H*5), 6.30 (bs, 1H, NH), 5.05 (m, 1H, CH_2NH), 4.31−3.96 (m, 3H, CH_2-NH), 3. 70 (m, 2H, nbd C*H*), 3.46−3.42 (m, 2H, *H*C═CH), 3.44, (s, 3H, Py*Me*), 2.96 (m, 2H, HC═C*H*), 1.14 (m, 2H, nbd CH_2). ^{13}C NMR (75 MHz, [D_6]acetone, 298 K): δ 163.0 (PyMe *C*2), 160.2 (Py *C*2), 157.1 (PyMe *C*6), 147.7 (Py *C*6), 138.3 (PyMe *C*4), 138.2 (Py *C*4), 124.1 (Py *C*3), 124.0 (Py *C*4), 121.7 (PyMe *C*5), 120.3 (PyMe *C*3), 58.5(*C*H_2NH), 58.4 (*C*H_2NH), 58.2 (nbd *C*H_2), 48.2 (nbd *C*H),40.0 (nbd ═*C*), 37.9 (nbd ═*C*), 27.6 (Py*Me*). ESI-MS (*m*/*z*): 408 ([**1**]$^+$). Anal. Calcd for $C_{20}H_{23}N_3RhPF_6$: C, 43.42; H, 4.19; N, 7.59. Found: C, 43.25; H, 4.21; N, 7.64.

(25) (a) *PQS* version 2.4; Parallel Quantum Solutions: Fayetteville, AR, 2001 (the Baker optimizer is available separately from PQS upon request). (b) Baker, J. *J. Comput. Chem.* **1986**, *7*, 385.

(26) (a) Becke, A. D. *Phys. Rev. A* **1988**, *38*, 3089. (b) Perdew, J. P. *Phys. Rev. B* **1986**, *33*, 8822.

(27) (a) Lee, C.; Yang, W.; Parr, R. G. *Phys. Rev. B* **1988**, *37*, 785. (b) Becke, A. D. *J. Chem. Phys.* **1993**, *98*, 1372. (c) Becke, A. D. *J. Chem. Phys.* **1993**, *98*, 5648. (d) All calculations were performed using the Turbomole functional "b3-lyp", which is not identical to the Gaussian "B3LYP" functional.

Downloaded by NAT LIB UKRAINE on July 6, 2009
Published on July 28, 2004 on http://pubs.acs.org | doi: 10.1021/om049654x

Synthesis of [(η^4-Norborna-1,4-diene)-(η^3-fac-*N*-(2-pyridylmethyl)-*N*-(6-methyl-2-pyridylmethyl)amine)rhodium(II)] Bishexafluorophosphate ([1]$(PF_6)_2$). Treatment of a 6 mL solution of [**1**]PF_6 (509 mg) with 1 equiv of $AgPF_6$ (235) in acetone yields a dark green solution of [**1**]$(PF_6)_2$ and a black precipitate. The solution was filtrated and subsequently added to 25 mL of diethyl ether. A dark green oil of [**1**]$(PF_6)_2$ was obtained, which was evaporated, yielding a dark green foam. The solid was washed with diethyl ether, yielding a precipitate of [**1**]$(PF_6)_2$ (310 mg/48% yield). Magn. sus.: $\mu_{eff} = 1.6\ \mu_B$. Anal. Calcd for $C_{20}H_{23}N_3RhP_2F_{12}\cdot C_3H_6O$: C, 34.35; H, 3.98; N, 5.72. Found: C, 34.04; H, 3.91; N, 5.90.

Synthesis of *R,R*-[{(η^1-3-Hydroxynorborn-5-en-2-yl)-(η^3-mer-*N*-(2-pyridylmethyl)-*N*-(6-methyl-2-pyridylmethyl)amine)-(μ_2-chloride)rhodium(III)}$_2$] Bishexafluorophosphate and *R,S*-[{(η^1-3-Hydroxynorborn-5-en-2-yl)-(κ^3-mer-*N*-(2-pyridylmethyl)-*N*-(6-methyl-2-pyridylmethyl) amine)-(μ_2-chloride)rhodium(III)}$_2$] Bishexafluorophosphate ([2a]$(PF_6)_2$ and [2b]$(PF_6)_2$). To a solution of 426 mg of [**1**]PF_6 in 4 mL of acetone was added an excess of $FeCl_3$ in 4 mL of water. After stirring for 4 h a 1:1 mixture of [**2a**]$(PF_6)_2$ and [**2b**]$(PF_6)_2$ had precipitated from the solution. The precipitate was filtrated, washed with water and diethyl ether, and dried in vacuo (326 mg/70% yield). ^{1}H NMR (200 MHz, [D_6]acetone, 298 K): δ 8.40 (m, 0.5H, Py *H*6), 8.28 (m, 0.5H, Py *H*6), 8.1−7.9 (m, 2H, Py *H*4, MePy *H*4), 7.7−7.5 (m, 1H, Py *H*3), 7.48 (m, 1H, MePy *H*3), 7.3−7.1 (m, 1H, MePy *H*5), 6.8−7.1 (m, 1H, Py *H*5), 6.5 (m, 1H, N*H*), 5.97 (m, 1H, nbd *H*6), 5.68 (m, 1H, nbd *H*2), 5.5−4.9 (m, 5H, CH_2NH, nbd *H*5), 4.05 (m, 0.5H, nbd *H*3), 3.55 (d, $^3J_{H,H} = 4.2$ Hz, 0.5H, nbd *H*3), 2.64 (m, 0.5H, nbd *H*4), 2.53 (m, 0.5H, nbd *H*4), 2.41 (m, 1H, nbd *H*1), 2.4−2.1 (m, 3H, Py*Me* and some impurities), 1.83 (d, $^3J_{H,H} = 8.2$ Hz, 1H, nbd *H*7), 1.30 (m, 1H, nbd *H*7). Because most of the signals of [**2a**]$^{2+}$ and [**2b**]$^{2+}$ overlap, it was not possible to distinguish between the signals for [**2a**]$^{2+}$ and [**2b**]$^{2+}$. Assignment of the NMR signals is in accordance with the atom labeling in Figure 4. We were not able to assign the O*H* proton. ESI-MS (*m*/*z*): 424 ([(Me-dpa)(η^1-hydroxynorbornenyl)(Cl) $Rh^{III}]^+$ − HCl), 460 ([(Me-dpa)(η^1-hydroxynorbornenyl)(Cl) $Rh^{III}]^+$). The μ_2-chloride bridges easily break and only monocationic, monomeric fragments of [**2**]$^{2+}$ are observed in the ESI-MS. Calculated for [(Me-dpa)(η^1-hydroxynorbornenyl)(Cl)$Rh^{III}]^+$ ($C_{20}H_{24}N_3ORhCl$): *m*/*z* 460.06559. Found: 460.06819 ($\Delta = -5.7$ ppm).

[(η^1-3-Hydroxynorborn-5-en-2-yl)-(κ^3-mer-*N*-(2-pyridylmethyl)-*N*-(6-methyl-2-pyridylmethyl)amine)-(chloride)-(dimethylformamide)rhodium(III)] Hexafluorophosphate (mononuclear DMF adduct of [2]$^{2+}$). The mononuclear DMF adduct of [**2**]$^{2+}$ was obtained by dissolving [**2**]$^{2+}$ in DMF. This results in a mixture of two mass-identical isomers (probably as a result of exchange of DMF and Cl^- positions). NMR data are only reported for the major component (which obscure most of the signals from the minor component). ^{1}H NMR main product (200 MHz, [D_7]dimethylformamide, 298 K): δ 9.06 (m, 1H, Py *H*6), 8.0−7.8 (m, 2H, Py *H*4, MePy *H*4), 7.6−7.3 (m, 4H, Py *H*3, *H*5, MePy, *H*3, *H*5), 6.01 (bs, 1H, N*H*), 5.92 (m, 1H, nbd *H*6), 5.4−4.5 (m, 5H, CH_2NH, nbd *H*2, nbd *H*5), 3.09 (s, 3H, *Me*Py), 1.92 (m, 1H, nbd *H*7), 1.32 (m, 1H, nbd *H*7). Assignment of the NMR signals is in accordance with the atom labeling in Figure 4 (the signals of nbd *H*3 and *H*6 are probably obscured by the signals of DMF). ^{13}C NMR (75 MHz, [D_7]dimethylformamide, 298 K): δ 165.9, 164.8, 164.0, 152.5, 152.4, 138.9, 138.5,137.8, 134.7, 126.1, 123.9, 121.8, 119.3, 77.8, 59.7, 59.3, 58.5, 58.2, 46.9, 27.8. ESI-MS (*m*/*z*): 533 ([(Me-dpa)(η^1-hydroxynorbornenyl)(Cl)(DMF)$Rh^{III}]^+$).

Synthesis of *R,R*-[{(η^1-3-Methoxynorborn-5-en-2-yl)-(κ^3-mer-*N*-(2-pyridylmethyl)-*N*-(6-methyl-2-pyridylmethyl)amine)-(μ_2-chloride)rhodium(III)}$_2$] Bishexafluorophosphate and *R,S*-[{(η^1-3-Methoxynorborn-5-en-2-yl)-(κ^3-mer-*N*-(2-pyridylmethyl)-*N*-(6-methyl-2-pyridylmethyl)-amine)-(μ_2-chloride)rhodium(III)}$_2$] Bishexafluorophosphate ([3a]$(PF_6)_2$ and [3b]$(PF_6)_2$). To 300 mg of [Rh(nbd)Cl]$_2$ was added 5 mL of methanol, which was distilled over $CaSO_4$. A small excess of Me-dpa was added, and the reaction mixture was stirred until an orange solution was obtained. To the solution was added 400 mg of [Fc]PF_6, yielding a gray precipitate after several hours. The gray product was filtrated, washed with methanol, and extracted with acetone, yielding a yellowish solution of [**3**]$(PF_6)_2$ in acetone. A yellow powder of 180 mg (17% yield) consisting of a 2:1 mixture of [**3a**]$^{2+}$ and [**3b**]$^{2+}$ was obtained by evaporation of acetone. Traces of [**5**]$^{2+}$, and when aqueous methanol was used also [**2**]$^{2+}$, were always present. Recrystallization from acetone/dioxane yields crystals suitable for X-ray diffraction. ^{1}H NMR (200 MHz, [D_6]acetone, 298 K): δ 8.34 (d, $^3J_{H,H} = 5.5$ Hz, 0.5H, Py *H*6), 8.21(d, $^3J_{H,H} = 5.8$ Hz, 0.5H, Py *H*6), 8.12−7.90 (m, 2H, Py *H*4, MePy *H*4), 7.77−7.54 (m, 1H, Py *H*3), 7.43 (d, $^3J_{H,H} = 7.7$ Hz, 1H, MePy *H*3), 7.24−6.83 (m, 2H, MePy *H*5, Py *H*5), 6.00 (m, 2H, nbd *H*6), 5.22−4.75 (m, CH_2NH, nbd *H*5, *H*2, *H*3), 3.00 (s, 3H, O*Me*), 2.76 (bs, 1H, nbd *H*4), 2.59 (bs, 1H, nbd *H*1), 2.27 (s, 3H, *Me*Py), 1.68 (d, $^3J_{H,H} = 8.4$ Hz, 1H, *H*7), 1.24 (m, 1H, *H*7). The signals of NH could not be assigned and are probably obscured by other signals. As most of the signals of [**3a**]$^{2+}$ and [**3b**]$^{2+}$ overlap, it was not possible to distinguish between the signals belonging to [**3a**]$^{2+}$ and [**3b**]$^{2+}$. Assignment of the ^{1}H NMR signals is in accordance with the atom labeling in Figure 4. Due to the low solubility of [**3**]$^{2+}$ in weakly coordinating solvents such as acetone, we were not able to obtain satisfactory ^{13}C NMR spectra of this compound ([**3**]$^{2+}$ rearranges to an unidentified mixture of mononuclear compounds in stronger coordinating solvents such as DMF). ESI-MS (*m*/*z*): 438 ([(Me-dpa)(η^1-methoxynorbornenyl)(Cl) $Rh^{III}]^+$ − HCl), 474 ([(Me-dpa)(η^1-methoxynorbornenyl)(Cl) $Rh^{III}]^+$). The μ_2-chloride bridges easily break and only monocationic, monomeric fragments of [**3**]$^{2+}$ are observed in the ESI-MS. Calculated for [(Me-dpa)-(η^1-methoxynorbornenyl)(Cl)$Rh^{III}]^+$ ($C_{21}H_{26}N_3ORhCl$): *m*/*z* 474.08124. Found: *m*/*z* 474.07828 ($\Delta = 6.2$ ppm).

Synthesis of *R,R*-[{(η^1-Norborn-5-en-2-yl)-(κ^3-mer-*N*-(2-pyridylmethyl)-*N*-(6-methyl-2-pyridylmethyl)amine)-(μ_2-chloride)rhodium(III)}$_2$] Bishexafluorophosphate and *R,S*-[{(η^1-Norborn-5-en-2-yl)-(κ^3-mer-*N*-(2-pyridylmethyl)-*N*-(6-methyl-2-pyridylmethyl)amine)-(μ_2-chloride)rhodium(III)}$_2$] Bishexafluorophosphate ([5a]$(PF_6)_2$ and [5b]$(PF_6)_2$). To a suspension of [**1**]PF_6 (243 mg) in 6 mL of methanol was added 0.5 mL of concentrated chloride acid, yielding immediately a light-yellow/colorless solution. After standing for 1 day a yellow precipitate of a 1:1 mixture of [**5a**]-$(PF_6)_2$ and [**5b**]$(PF_6)_2$ had crystallized from the solution (140 mg/72% yield). Crystals suitable for X-ray diffraction of [**5a**]-$(PF_6)_2$ and [**5b**]$(PF_6)_2$ were obtained by partial evaporation of a solution of [**5**]$^{2+}$ in DMF and subsequent recrystallization from acetone/dioxane. ^{1}H NMR (200 MHz, [D_6]acetone, 298 K): δ 8.53 (d, $^3J_{H,H} = 4.6$ Hz, 0.5H, Py *H*6), 8.41 (d, $^3J_{H,H} = 4.9$ Hz, 0.5H, Py *H*6), 8.2−7.9 (m, 2H, Py *H*4, MePy *H*4), 7.72 (m, 1H, Py *H*3), 7.50 (d, $^3J_{H,H} = 6.4$ Hz, 1H, MePy *H*3), 7.26 (d, $^3J_{H,H} = 6.4$ Hz, 0.5H, MePy *H*5), 7.15 (d, $^3J_{H,H} = 9.2$ Hz, 0.5H, MePy *H*5), 7.2−7.0 (m, 1H, Py *H*5), 6.07 (m, 1H, nbd *H*6), 5.54 (bs, 1H, N*H*), 5.3−4.7 (m, 5.5H, CH_2NH, nbd *H*5, *H*2), 4.63 (m, 0.5H, nbd *H*5), 2.70 (bs, 1H, nbd *H*4), 2.58 (bs, 1H, nbd *H*1), 2.26 (s, 1.5H, *Me*Py), 2.18 (s, 1.5H, *Me*Py), 1.46 (m, 1H, nbd *H*3-*anti*), 1.35 (d, $^3J_{H,H} = 7.0$ Hz, 1H, nbd *H*7 *rhodium side*), 1.07 (m, 1H, nbd *H*7 *olefin side*), −0.17 (m, 1H, nbd *H*3-*syn*). As most of the signals of [**5a**]$^{2+}$ and [**5b**]$^{2+}$ overlap, it was not possible to distinguish between the signals of [**5a**]$^{2+}$ and [**5b**]$^{2+}$. Assignment of the NMR signals is in accordance with the atom labeling in Figure 5. ESI-MS (*m*/*z*): 408 ([(Me-dpa)(η^1-norbornenyl)(Cl) $Rh^{III}]^+$ − HCl), 444 ([(Me-dpa)(η^1-norbornenyl)(Cl) $Rh^{III}]^+$). The μ_2-chloride bridges easily break and only monocationic, monomeric fragments of [**5**]$^{2+}$ are observed in the ESI-MS. Calculated for [(Me-dpa)(η^1−norbornenyl)-(Cl)$Rh^{III}]^+$ ($C_{20}H_{24}N_3RhCl$): *m*/*z* 444.07068. Found: *m*/*z* 444.06723 ($\Delta = 7.8$ ppm). Anal. Calcd for $C_{40}H_{48}N_6O_2Rh_2$-

$Cl_2P_2F_{12}$·CH_4O: C, 40.55; H, 4.34; N, 6.75. Found: C, 40.29; H, 4.34; N, 6.52.

[(η^1-Norborn-5-en-2-yl)-(κ^3-mer-*N*-(2-pyridylmethyl)-*N*-(6-methyl-2-pyridylmethyl)amine)-(chloride)-(dimethylformamide)rhodium(III)] Hexafluorophosphate (mononuclear DMF adduct of [5]$^{2+}$). The mononuclear DMF-adduct of [**5**]$^{2+}$ was obtained by dissolving [**5**]$^{2+}$ in DMF. ^{1}H NMR (200 MHz, [D_7]dimethylformamide, 298 K): δ 9.15 (m, 1H, Py *H*6), 8.1−7.9 (m, 2H, Py *H*4, MePy *H*4), 7.6−7.4 (m, 4H, Py *H*3, *H*5, MePy, *H*3, *H*5), 6.13 (m, 1H, nbd *H*6), 5.5 (bs, 1H, N*H*), 5.4−4.4 (m, 5H, CH_2NH, nbd *H*2, nbd *H*5), 3.07 (s, 3H, *Me*Py), 1.5−1.0 (m, 3H, nbd *H*3-*anti*, nbd *H*7), −0.08 (m, 1H, nbd *H*3-*syn*). Assignment of the NMR signals is in accordance with the atom labeling in Figure 5 (the signals of nbd *H*3 and *H*6 are probably obscured by the signals of DMF). ^{13}C NMR (75 MHz, [D_7]dimethylformamide, 298 K): δ 166.3, 165.0, 164.3, 160.1, 151.9, 139.2, 139.0, 138.3, 132.8, 125.67, 124.1, 121.3, 119.9, 59.7, 58.6, 50.8, 50.1, 41.5, 32.4, 26.5. ESI-MS (*m*/*z*): 517 ([(Me-dpa)(η^1-norbornenyl)(Cl)(DMF)Rh^{III}]$^+$).

Acknowledgment. This work was supported by the Netherlands Organisation for Scientific Research (NWO-CW). We thank Dr. Peter H. M. Budzelaar for helpful tips and tricks concerning the DFT calculations, Paul P. J. Schlebos for measuring the 2D NMR measurements, and Theo P. J. Peters for his assistance with the synthesis of the Me-dpa ligand.

Supporting Information Available: X-ray crystallographic file in CIF format for the structure of compounds [**1**]-PF_6, [**2**]$(BPh_4)_2$, and [**5**]$(PF_6)_2$. This material is available free of charge via the Internet at http://pubs.acs.org.

OM049654X

Downloaded by NAT LIB UKRAINE on July 6, 2009
Published on July 28, 2004 on http://pubs.acs.org | doi: 10.1021/om049654x